Association of Metallurgical Engineers of Serbia *Review paper*
AMES *UDC:669.01.094.3/169.1-977=20*

HIGH TEMPERATURE OXIDATION OF METALS AND ALLOYS

IVAN ANŽEL

University of Maribor, Faculty of Mechanical Engineering (FME), Smetanova 17, 2000 Maribor, Slovenia

ABSTRACT

This article gives a general survey of high temperature oxidation in metals and alloys, demonstrating how different environmental conditions and chemical composition of the alloys determine the mode of oxidation process. As a special phenomenon, the internal oxidation wherein the oxygen atoms diffuse into the alloy and react with a less-noble solute element is also reviewed. The basic knowledge, the models and understanding of the phenomena are summarized from the literature which is written at the end of the paper.

Key words: High temperature oxidation, internal oxidation, mechanisms, models

1. THE MODELS AND MECHANISMS OF HIGH TEMPERATURE OXIDATION

There are, with the exception of gold, no pure metals or alloys stable in air at room temperature. All metals tend to form oxides although in many instances the rate of reaction is very slow at low temperatures. Reaction rates increase rapidly with any increase in temperature, and at very high temperatures most reactions are completed within a few minutes. Therefore, depending on the equilibrium conditions, oxygen-metal reactions are almost always likely to occur, and oxidation problems are mostly reduced to determining the reaction rate.

Many different effects can occur during oxidation of the alloy composed of the base metal *M* and alloying element *B*. Progression of the process depends on the alloy's composition, environmental conditions (T, Po_2), and other influencing parameters. The most important are:

- Free energy of oxide formation ($\Delta G_f^{MO_m}, \Delta G_f^{BO_n}$)

- Their relative difference ($\Delta G = \Delta G_f^{MO_m} - \Delta G_f^{BO_n}$)

- Maximum solubility of oxygen in the base metal (C_O^{max})

- Concentration of alloying element (C_B^0)

Basically, high temperature oxidation can be divided into two limited procedures:

1. Oxidation processes where oxygen atoms do not dissolve in the base metals;

2. Oxidation processes where the base metal exhibits solubility for oxygen.

In the first case reaction begins at the metal/gas interface and this reaction's products form an intermediate layer between the alloy and the gas. The possible forms this layer can create are numerous; and the form may even alter as the reaction progresses. In order for the reaction to proceed further, one or both reactants must penetrate the scale, i.e. either metal must be transported through the oxide to the oxide/gas interface and react there, or oxygen must be transported to the oxide/metal interface and react there. The mechanisms by which the reactants may penetrate the oxide layer are an important part of the mechanism by which high temperature oxidation occurs. Since all metal oxides are ionic in nature, it is clear that ions and electrons must migrate in order for the reaction to proceed. The transporting step of the reaction's mechanism links the two-phase boundary reactions, as can be seen in Figure 1.

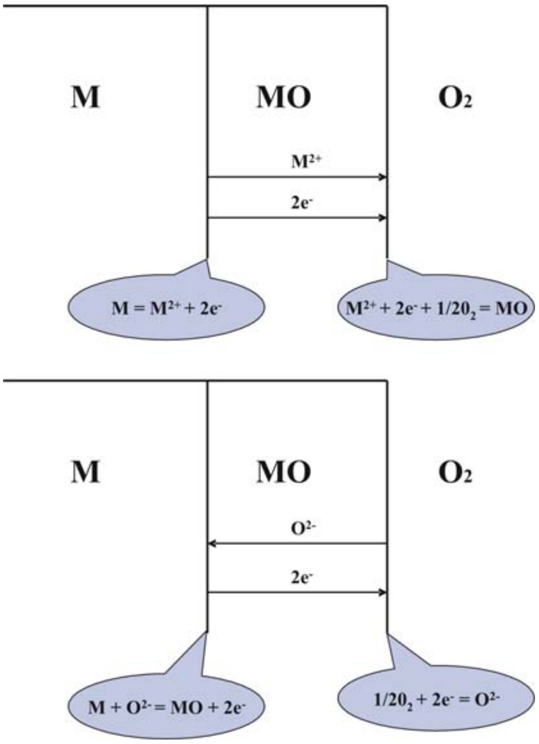

Figure 1: Interfacial reactions and transport processes for high temperature oxidation mechanisms: (a) cation mobile (b) anion mobile

An important distinction should be made between scale growth by (predominantly) cation migration, and scale growth by anion migration. Cation migration leads to scale formation at the scale/gas interface, whereas anion migration leads to scale formation at the metal/scale interface. In order to achieve simultaneous migration of ions and electrons it is necessary that the oxides formed during oxidation are non-stoichiometric compounds (the metal to non-metal atom ratio is not exactly that given by the chemical formula, even though the compound is electrically neutral; either the anion or the cation must exhibit variable valency on its sub-lattice).

In the next Figures (2-4) three relatively simple possibilities for forming oxide layers are selected. In Figure 2, shows an oxidation process for the alloy composed of base metal M and alloying element *B*. The atoms of *B* may form two oxides BO_n and BO_m (m>n) as two coherent layers, which are considered to be free of mechanical imperfections. *B* is less noble than *M* so that it will oxidize preferentially. Single steps that may occur in this type of oxidation are as follows:

- Diffusion of *B* within the alloy;
- Ionization of *B* to form B^{2n+} and electrons;
- Diffusion of B^{2n+} and electrons in the BO_n layer;
- Further ionization of B^{2n+} to B^{2m+} ions and electrons;
- Diffusion of B^{2m+} ions and electrons in the *BOm* layer;
- Adsorption of oxygen at the oxide-oxygen interface;
- Ionization of the adsorbed oxygen;
- Diffusion of O^{2-} in the BO_m layer;
- Reaction between B^{2n+} and O^{2-};
- Diffusion of O^{2-} in the BO_n layer.

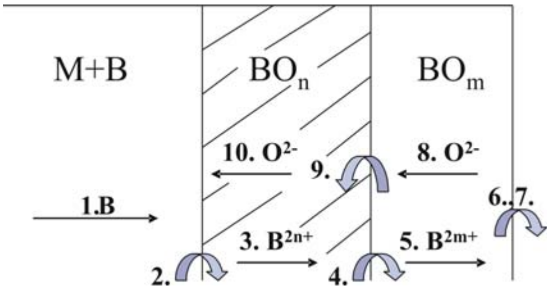

Figure 2: The model of oxidation process with continuously formed oxide layers of alloying element

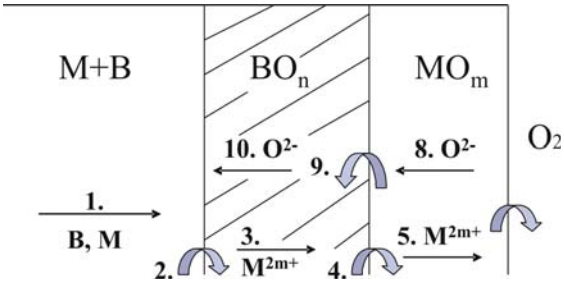

Figure 3: The model of oxidation process with continuously formed oxide laye of alloying element and base metal

For complex reactions of this kind, in which alternative routes lead to the same result, the fastest route is the one that determines the rate. For example the latter process may be neglected, if the positive *B* ions travel much faster than the negative oxygen ions in the opposite direction. On the other hand, the overall rate of an individual route (chemical reaction) which proceeds over several simple successive steps is determined by the rate of the slowest step. From the practical aspect, we always have to decrease the rate of the slowest step in order to retard the overall reaction rate.

In Figure 3 the element B is again considered to be lesser noble than the two metals, and may preferentially build-up an oxide BO_n at the alloy's surface. If B is present in the alloy as a small percentage, this reaction may almost stop owing to the impoverishment of B in the outer parts of the alloy specimen. Further reaction would then occur by oxidation of the second metal, M, to form MO_m on top of BO_n. In this case, some steps of the reaction are similar to that of Figure 2. The main difference between mechanisms 1 and 2 is that, in case 1 the metal ions pass through cation lattices of their own kind, while in case 2 they also pass through the cation lattice of another metal. For this, M ions must be soluble to a certain extent in BO_n. Valency M^{2m+} represents only one possibility; *the* M ions should also assume another valency (M^{2n+} for example).

In a third possibility for the surface reaction of a binary alloy in oxygen, as indicated by Figure 4, the surface oxides do not form a coherent layer. The holes shown in the sketch may consist of pores, cracks, or channels of any shape, obviously having little protective action on the underlying metal surface. In this case, diffusion in the oxide layer need not be considered, since oxygen reaches the metal surface more rapidly than the diffusion takes place. Reaction occurs at the metal-oxide interface, and the oxide, being built up from the bottom, will be pushed away from the surface.

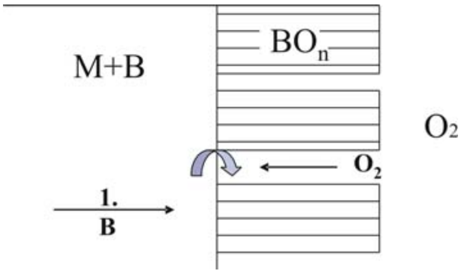

Figure 4: The model of oxidation process where the oxide of alloying element does not form a continuous layer

In the second case, we consider the following situation: A small quantity of a less noble alloying element B is present in the base metal M which exhibits solubility for oxygen, and the alloy is exposed to the atmosphere oxidising for both alloying elements. At the high temperature oxidation, morphology can be formed, as illustrated in Figure 5.

Oxidation starts with dissolution of oxygen into the surface layer. When the concentration of oxygen in the surface layer reaches equilibrium concentration for the oxidation of less-noble alloying element, the reaction occurs and solute oxide starts to grow on the surface. The possible forms and mechanisms of the layer's growth are the same as for first case. As previously explained, oxidation starts with dissolution of oxygen into the lattice of the base metal. Consequently, a concentration gradient is created (developed) and oxygen atoms diffuse inward throughout the alloy. At an individual position, the concentration of oxygen increases over time and, again, when the equilibrium concentration for oxidizing the solute element is obtained the reaction occurs and oxide particles BO_n precipitate from the solid solution (matrix α_M), This process has the name "internal oxidation" and the layer, composed of oxide particles precipitated in a matrix is called "subsurface" or the "internal oxidation zone". Of course, if the oxygen pressure is low enough (the partial pressure of oxygen in the atmosphere must be equal or lower than the equilibrium pressure for oxidation of base metal) it is possible to produce the subscale only, without the formation of external layers of the base metal oxide (Figure 6). The metal surface remains bright and clean while oxidation is occurring, in fact, within the base metal. The border of the Internal Oxidation Zone (IOZ) presents the reaction (oxidation) front. This is the position of the latest oxide particles' precipitation. In the surface layer, dissolved oxygen constantly diffuses inward through the IOZ and provides the necessary oxygen concentration for continuous precipitation of the oxide particles at the reaction front. When the metallic solute is exhausted at the reaction front, oxygen diffuses further into the alloy and thus increases the thickness of the internal oxidation zone.

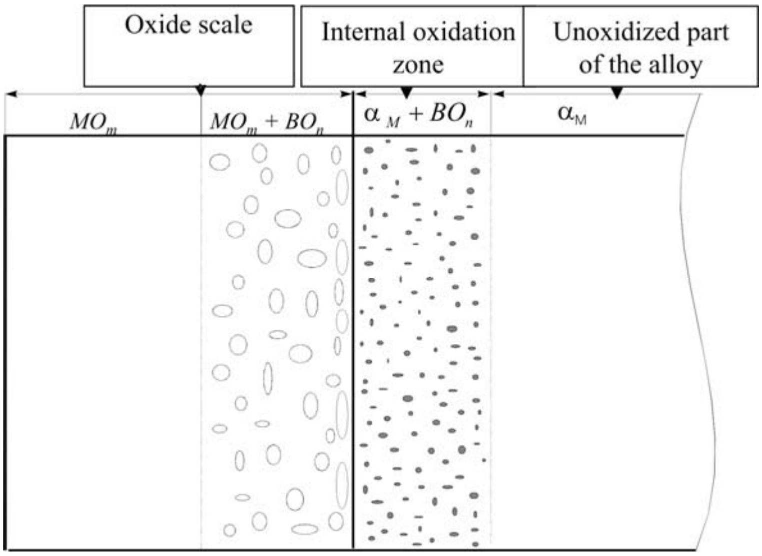

Figure 5: Schematic diagram of the oxidation morphology of dilute M-B alloy at $p_{O_2} > p_{O_2}^{M/MO_m}$

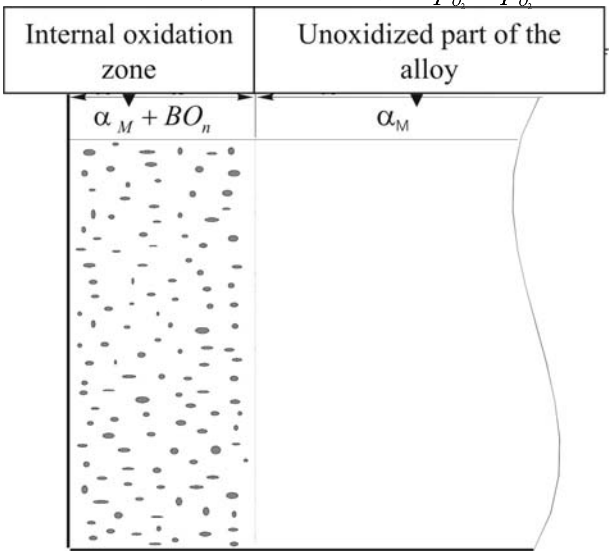

Figure 6: Schematic diagram of the oxidation morphology of dilute M-B alloy at $p_{O_2} \leq p_{O_2}^{M/MO_m}$

2. NECESSARY CONDITIONS FOR THE INTERNAL OXIDATION PROCESS

Some basic conditions have to be satisfied for the internal oxidation process in alloy M-B:

- Free-energy formation (per mole of oxygen) for the solute metal oxide must be more negative than the free energy formation (per mole of oxide) of the base metal (lowest oxide): $\left|\Delta G_f^{BO_n}\right| > \left|\Delta G_f^{MO_m}\right|$
- Free-energy change for the reaction of dissolved oxygen with solute to form solute metal oxide in the solvent lattice must be negative:

$$[B]_M + n[O]_M \rightarrow BO_n \qquad \Delta G < 0 \tag{1}$$

Therefore, at the oxidation temperature, the base metal must exhibit enough high solubility and diffusivity for sufficient oxygen to establish the required activity of the dissolved oxygen atoms at the reaction front (dissolved concentration of oxygen must present an oxidizing atmosphere for the alloying element B in the matrix solid solution – α_M).

- Diffusivity of oxygen in the solid solution (α_M) must be greater than the diffusivity of the alloying element *(*$D_O > D_M$*),* if not, the oxidation process occurs only at the free-surface. Namely, because of faster diffusion of the solute atoms their concentration in the surface layer never drops to zero (B atoms are never exhausted), and oxygen atoms cannot diffuse further into the alloy.
- The solute concentration of the alloy must be lower than that required for transition from internal to external oxidation. Precipitated oxide particles present obstacles for oxygen diffusion. It exists the critical concentration of alloying element where the volume fraction of precipitated oxide at the internal oxidation front increases to a value that prevents further diffusion of oxygen into the non-oxidized part of the alloy.
- No surface layer must prevent the dissolution of oxygen into the alloy at the start of oxidation.

3. THE MECHANISM OF INTERNAL OXIDATION

The process of internal oxidation can be divided into several steps:

- Adsorption - the reactant gas molecules must approach the metal surface and become adsorbed there**.**
- The adsorbed molecules then split to form adsorbed oxygen atoms.
- Dissolution of the oxygen into the lattice of the base metal at the external surface (oxygen atoms occupy interstitial sites in the lattice of the base metal).
- Diffusion of dissolved oxygen inward through the base metal matrix. Increasing oxygen concentration in the surface layer creates a concentration gradient and diffusion of oxygen atoms inward to the internal oxidation front.

- Reaction of the oxygen atoms with the atoms of alloying element at the internal oxidation front, and precipitation of the oxide particles from the solid solution.

At the internal oxidation front prevails a local thermodynamic equilibrium and the circumstances at this place are interpreted by the ternary phase diagram M-B-O (Figure 7). The equilibrium oxygen concentrations lie on line E-F for the oxide BO_n and the equilibrium concentration is obtained at the point P1 for the selected alloy C_B^1.

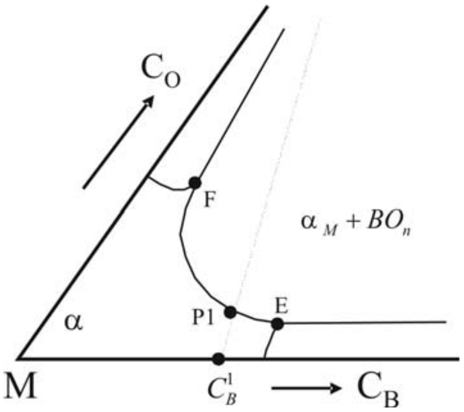

Figure 7: Isothermal section through the ternary phase diagram M-B-O at the internal oxidation temperature

The next Figure 8 shows the situation at distance X from the alloy surface, which is the place of the oxide particles next precipitation (Figure 8).

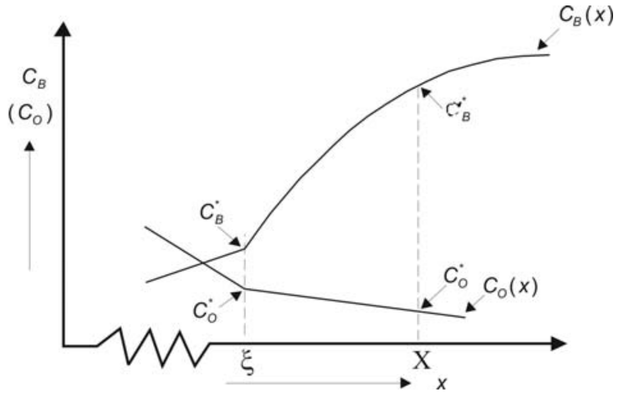

Figure 8: Concentration profiles in the vicinity of the precipitation front

The reaction proceeds at the internal oxidation front (ξ) and the concentrations of reactive elements $C_B^{'}$ and $C_O^{'}$ correspond (oxygen and element B) to the equilibrium solubility product, which is defined as

$$K_{sp}^{BO_n} = \left(C_B^{'}\right) \cdot \left(C_O^{'}\right)^n \qquad (2)$$

Diffusion from the outer region increases the concentration of oxygen in the solid solution at both places. At a constant flux of oxygen to the internal oxidation front, the quantity which is consumed during the reaction continuously decreases over time - the rest of the alloying element's concentration and the oxygen concentration increase at both positions.

At the appointed oxygen concentration (depending on the concentration of the alloying element) the solubility product ($K_{sp}^{BO_n}$) is obtained but the precipitation still does not occur. With further increase of oxygen concentration we arrive at a two-phase region (α_M + BO_n) in the isothermal section of equilibrium ternary-phase diagram. The oxide precipitates after the attainment of critical supersaturation for homogeneous precipitation ($S_{hom}^{BO_n} = \left(C_B^*\right) \cdot \left(C_O^*\right)^n / K_{sp}^{BO_n}$). According to the classical nucleation theory, the activation barrier to nucleation (G*) can be estimated from the free-energy change for the formation of a nucleus of radius r:

$$\Delta G = 4\pi r^2 \sigma + 4/3\,\pi r^3 \left(\Delta G_v + \Delta G_s\right) \tag{3}$$

where σ is the specific interfacial free-energy, (ΔG_v) is the free-energy change per unit volume of those precipitated particles formed during the reaction, and (ΔG_s) is the specific strain-energy.

4. THE KINETIC OF INTERNAL OXIDATION

The rate-controlling step for internal oxidation is diffusion of oxygen through the internal oxidation zone. If we neglect the influence of precipitated oxide particles in the IOZ on the diffusivity, the thickness of the internal oxidation zone (ξ) becomes a parabolic function of time, and can be expressed by the equation,

$$\xi = 2\gamma \left(D_O t\right)^{1/2} \tag{4}$$

and the velocity of the reactions front motion is then expressed as

$$d\xi / dt = \gamma \left(D_O / t\right)^{1/2} \tag{5}$$

where D_O is the diffusivity of oxygen in the base metal and y is a dimensionless parameter which depends on conditions during the internal oxidation process. Depending on the permeability of oxygen and the solute metal (the permeability is defined as a product of concentration and diffusivity - $C_{O(B)} \cdot D_{O(B)}$) we can define two limiting cases for determining the dimensionless parameter.

In the first case, when oxygen diffusion in the solvent is much more rapid than the solute diffusion, we can assume that:

- the reaction takes place only and completely at a sharp boundary plane between the internally-oxidized and the remaining part of the specimen
- the surface concentration of oxygen is practically equal to the solubility limit in the base metal at the internal oxidation temperature

- diffusion of alloying element can be neglected.

Figure 9 show the concentration profiles for oxygen and the solute element under these circumstances. To this case belong the alloys which satisfy the conditions that the ratio between the concentration of oxygen and alloying element, which is normally much lower than one, must be much greater than the ratio between the diffusivity of the alloying element and oxygen. According to requirements for the internal oxidation front, the flux of oxygen atoms arriving from the external surface must be equivalent to the flux of B atoms arriving from the bulk alloy

$$lim_{\varepsilon \to 0}\left[-D_O\left(\frac{\partial C_O}{\partial X}\right)_{X=\xi-\varepsilon} = nD_B\left(\frac{\partial C_B}{\partial X}\right)_{X=\xi+\varepsilon}\right] \tag{6}$$

(the concentrations profiles for oxygen and the solute element C_O, C_B are given by Fick's second law $\partial C/\partial t = D\,\partial^2 C/\partial X^2$).

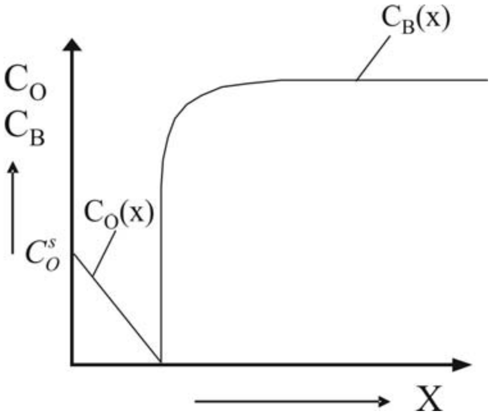

Figure 9: The concentration profiles of oxygen and solute element at the internal oxidation front for the case of neglected diffusion of alloying element

For a dimensionless parameter, we obtain the following solution

$$\gamma = \left[\frac{C_O^s}{2nC_B^0}\right]^{1/2} \tag{7}$$

and the equations for thickness of the IOZ and the velocity of the reaction front motion become,

$$\xi = \left(\frac{2C_O^s D_O}{nC_B^0}\cdot t\right)^{1/2} \tag{8}$$

$$\frac{d\xi}{dt} = \left(\frac{C_O^s D_O}{2nC_B^0 t} \right)^{1/2} \tag{9}$$

The last equation shows that the thickness increases with both increasing oxygen concentration, and diffusivity but it is inversely-proportional to the solute concentration.

In the second limiting case, the rate of the alloying element's outward diffusion as, well as the rate of inward oxygen diffusion are important in determining the kinetics of oxidation. In this case $C_O^s / C_B^0 << D_B / D_O << 1$ we have solute enrichment in the zone of internal oxidation (Figure 10). The dimensionless parameter then becomes equal

$$\gamma = \left(\frac{\pi^{1/2} \Phi^{1/2} C_O^s}{2nC_B^0} \right) \tag{10}$$

where $\Phi = D_O / D_B$.

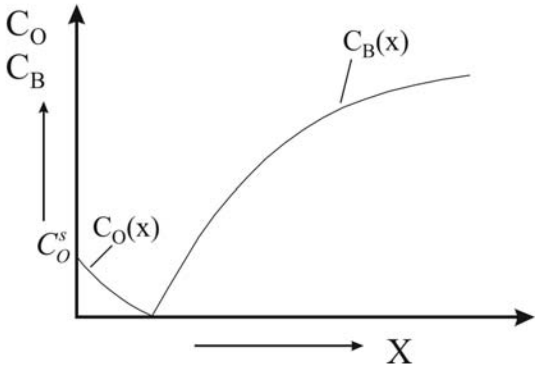

Figure 10: The concentration profiles of oxygen and solute element at the internal oxidation front for the case where diffusion of alloying element has to be considered

Acknowledgement

Many thanks are offered to my colleague dr. Rebeka Rudolf, who assisted and managed the preparation of this article.

REFERENCES

[1] C. Wagner, *Z. Electrochem.* **63** , 772 (1959).

[2] R.A. Rapp, *Corrosion* **21**, 382 (1965).

[3] Meijering, J.L., in: M. Herman (Ed.), Advances in Materials Research, Vol. 5, John Willey, New York (1970) 1.

[4] Pastorek, R.L.; Rapp, R.A.: Trans. Metall. Society of AIME 245 (1969) 1711.

[5] D.L. Douglass, *Oxid. Met.* **44**, 81 (1995).

[6] F. Gesmundo and B. Gleeson, *Oxid. Met.* **44**, 211 (1995).

[7] ANŽEL, Ivan, KNEISSL, Albert C., KOSEC, Ladislav, KRIŽMAN, Alojz. Internal oxidation of rapidly solidified Cu-Zr alloys. *Z. Met.kd.*, 1997, bd. 88, heft 1, p. 38-44. [COBISS.SI-ID 2494486]

[8] ANŽEL, Ivan, KNEISSL, Albert C., KOSEC, Ladislav. Internal oxidation of rapidly solidified ternary copper alloys. Part I, A new model of dispersoids formation. *Z. Met.kd.*, 1999, bd. 90, heft 8, p. 621-629. [COBISS.SI-ID 4718358]

[9] ANŽEL, Ivan, KNEISSL, Albert C., KOSEC, Ladislav. Internal oxidation of rapidly solidified ternary copper alloys. Part II, An experimental study. *Z. Met.kd.*, 1999, bd. 90, heft 8, p. 630-636. [COBISS.SI-ID 4719382]

[10] ANŽEL, Ivan, KNEISSL, Albert C. Formation of disperoids during internal oxidation of rapidly solidified Cu-Al-Zr alloys. *Adv. eng. mater. (Print)*, 2000, vol. 2, no. 10, p. 658-662. [COBISS.SI-ID 5903894]

[11] ANŽEL, Ivan. Dispersion strengthening of copper by internal oxidation of rapidly solidified Cu-Al-Zr alloys. *Metalurgija (Sisak)*, 2000, vol. 39, no. 4, p. 237-241. [COBISS.SI-ID 5646614]

[12] RUDOLF, Rebeka, ANŽEL, Ivan, KRIŽMAN, Alojz. Visokotemperaturna oksidacija kompozita Cu-C. *Mater. tehnol.*, 2001, vol. 35, no. 5, p. 219-226. [COBISS.SI-ID 6668054]

[13] KOSEC, Ladislav, ROTH, Jože, BIZJAK, Milan, ANŽEL, Ivan. Internal oxidation of an Ag-1.3at.%Te alloy. *Oxid. met.*, 2001, vol. 56, no. 5/6, p. 395-414. [COBISS.SI-ID 316511]

[14] ANŽEL, Ivan, KNEISSL, Albert C. Microstructure evolution during internal oxidation of copper-rare earth alloys = Gefügeentwicklung während der inneren Oxidation von Kupfer-Seltenerd-Legierungen. *Prakt. Metallogr.*, 2001, vol. 38, no. 11, p. 609-616. [COBISS.SI-ID 6694166]

[15] ANŽEL, Ivan, KNEISSL, Albert C., KRIŽMAN, Alojz, RUDOLF, Rebeka. Dispersion strengthening of copper by internal oxidation of rapidly solidified Cu-RE alloys. Part 1, The microstructure and stability of rapidly solidified ribbons. *Z. Met.kd.*, 2003,vol. 94, no. 2, p. 127-133. [COBISS.SI-ID 7761430]

[16] ANŽEL, Ivan, KNEISSL, Albert C., KOSEC, Ladislav, RUDOLF, Rebeka, GUSEL, Leo. Dispersion strengthening of copper by internal oxidation of rapidly solidified Cu-RE alloys. Part 2, Experimental study of internal oxidation. *Z. Met.kd.*, 2003, vol. 94, no. 9, p. 993-1000. [COBISS.SI-ID 8189718]

[17] ROTH, Jože, KOSEC, Ladislav, ŠKRABA, Polona, BIZJAK, Milan, MEDVED, Jože, DOBNIKAR, Meta, ANŽEL, Ivan. Internal oxidation of a Ag-1.3at.%Se alloy. Part I. Composition and Appearance of Oxidation Produces. *Oxid. met.*, October 2004, vol. 62, no. 3/4, p. 273-291 [COBISS.SI-ID 515167]

[18] ROTH, Jože, KOSEC, Ladislav, ANŽEL, Ivan. Internal oxidation of a Ag-1.3at.%Se alloy. Part II. Kinetics of internal oxidation. *Oxid. met.*, October 2004, vol. 62, no. 3/4, p. 293-308 [COBISS.SI-ID 515423]

[19] ANŽEL, Ivan, KOSEC, Ladislav, KNEISSL, Albert C. The creation of desired microstructures by internal oxidation. *Microsc. microanal. (Print)*. [Print ed.], 2005, vol. 11, suppl. 2, str. 1692-1693. http://journals.cambridge.org/ action/ display Fulltext?type=1&fid=325744&jid=&volumeId=&issueId=&aid=325743. [COBISS.SI-ID 9881878]

[20] RUDOLF, Rebeka, KOSEC, Ladislav, KRIŽMAN, Alojz, ANŽEL, Ivan. Microstructure analysis of internally oxidized Cu-C composite. *Metalurgija (Sisak)*, 2006, vol. 45, no. 2, p. 79-84. [COBISS.SI-ID 10111510]

[21] BRUNČKO, Mihael, ANŽEL, Ivan, KNEISSL, Albert C. In-situ monitoring of internal oxidation of dillute alloys. *Corros. sci.*. [Print ed.], Mar. 2007, vol. 49, no. 3, p.1228-1244. http://dx.doi.org/10.1016/j.corsci.2006.06.031. [COBISS.SI-ID 10702870]

[22] BRUNČKO, Mihael, KNEISSL, Albert C., ANŽEL, Ivan. Microstructural changes during internal oxidation of a Ag-Sn alloy = Gefügeänderungen wärhend der inneren Oxidation einer Ag-Sn Legierung. *Prakt. Metallogr.*, 2007, vol. 44, no. 10, p. 464-475. [COBISS.SI-ID 11772182]